

## **General Disclaimer**

### **One or more of the Following Statements may affect this Document**

- This document has been reproduced from the best copy furnished by the organizational source. It is being released in the interest of making available as much information as possible.
- This document may contain data, which exceeds the sheet parameters. It was furnished in this condition by the organizational source and is the best copy available.
- This document may contain tone-on-tone or color graphs, charts and/or pictures, which have been reproduced in black and white.
- This document is paginated as submitted by the original source.
- Portions of this document are not fully legible due to the historical nature of some of the material. However, it is the best reproduction available from the original submission.

X-621-69-158

PREPRINT

NASA TM X-63536

# THE GLOBAL STRUCTURE OF IONOSPHERE TEMPERATURE

L. H. BRACE

N 69-25557

(ACCESSION NUMBER)	(THRU)
<i>44</i>	
(PAGES)	
<i>Tmx 63536</i>	(CODE)
(NASA CR OR TMX OR AD NUMBER)	(CATEGORY)

MAY 1969



# **GODDARD SPACE FLIGHT CENTER**

## **GREENBELT, MARYLAND**

Paper A.1.5. presented at 12th Plenary Meeting of COSPAR,  
11-24 May, 1969  
Prague

X-621-69-158

THE GLOBAL STRUCTURE OF  
IONOSPHERE TEMPERATURE

by

L. H. Brace

May 1969

Goddard Space Flight Center  
Greenbelt, Maryland

PRECEDING PAGE BLANK NOT FILMED.

## CONTENTS

	<u>Page</u>
ABSTRACT . . . . .	v
INTRODUCTION . . . . .	1
THE EXPERIMENTAL METHOD . . . . .	3
THE OBSERVATIONS . . . . .	9
Pole-to-Pole Plots (1000 km) . . . . .	9
Local Time Behavior (1000 km) . . . . .	12
Solar Cycle Variations (1000 km) . . . . .	12
Polar Ionosphere at Solar Minimum (1000 km)	16
Winter Polar Ionosphere . . . . .	16
Summer Polar Ionosphere . . . . .	19
Diurnal Variation of Protonosphere $T_e$ (1000-3000 km) . . . . .	25
Latitudinal Structure of the Nightside Protonosphere (1000-3000 km)	28
DISCUSSION . . . . .	28
Processes Controlling $T_e$ . . . . .	28
Latitudinal Structure of $T_e$ . . . . .	32
Diurnal Variation in $T_e$ . . . . .	33
Nightside $T_e$ at low latitudes . . . . .	33
Diurnal Variation of $T_e$ at middle and high latitudes . . . . .	34
Solar Cycle Variation in $T_e$ . . . . .	35
CONCLUDING REMARKS . . . . .	36
ACKNOWLEDGEMENTS . . . . .	37
REFERENCES . . . . .	38

PRECEDING PAGE BLANK NOT FILMED.

THE GLOBAL STRUCTURE OF  
IONOSPHERE TEMPERATURE

by

L. H. Brace

ABSTRACT

The global pattern of electron temperature and its temporal behavior, as determined from satellite observations in the upper F-region and protonosphere, are described and discussed in terms of the processes which govern the electron thermal balance. The dayside temperature is greatest at middle latitudes ( $30^{\circ}$ - $50^{\circ}$  G.M.) while the nightside temperature peaks near  $60^{\circ}$  G.M. The temperatures over the polar cap are high at the summer pole, although not as high as daytime middle latitude temperatures. Temperatures over the winter pole are lower, but not as low as nighttime temperatures over the equatorial region. Much of this observed latitudinal structure and diurnal behavior can be understood in terms of a balance between photoelectron heating of the electrons, local cooling to ions and neutrals, and heat conduction within the electron gas. The variation of protonospheric heat capacity with field line length accounts for the different degrees of diurnal variation observed at the equator and at higher latitudes. The relatively low temperatures over the summer pole are attributed to the absence of an overlying protonosphere. The slightly elevated temperatures over the winter pole probably reflect non-ultraviolet sources of heating.

The onset of solar cycle effects were unexpectedly abrupt, with the electron temperature rising rapidly during 1965. A small decrease in daytime electron temperature has occurred since that time. The nighttime temperatures at low latitudes have continued to increase with the level of solar activity. This behavior can be attributed to basic changes in the atmospheric composition, density, and temperature and the effects of these upon the electron energy balance.

Measurements higher in the protonosphere ( $\approx$  3000 km) show that the temperature remains elevated all night at these levels. The energy conducted downward into the F-region at night varies from  $10^9$  eV cm $^{-2}$  sec $^{-1}$  at middle latitudes ( $60^\circ$  field tube) to  $10^8$  eV cm $^{-2}$  sec $^{-1}$  at low latitudes ( $35^\circ$  field tube). In the daytime similar amounts of heat are conducted downward at both middle and low latitudes.

## THE GLOBAL STRUCTURE OF IONOSPHERE TEMPERATURE

### INTRODUCTION

The accessibility to the ionosphere that has been provided in this decade by the advent of earth satellites has fostered extensive exploration of its global structure and its temporal behavior. The resolution of the electron temperature structure has thus far been far from complete because each satellite orbit tends to enhance certain kinds of spatial or temporal structure at the expense of other variations. For example, a purely polar, circular orbit enhances latitudinal resolution but completely suppresses altitudinal structure.

However, by combining the data from a number of satellites, it is now possible to assemble a reasonably good picture of the temperature patterns, at least at solar minimum. The response of the ionosphere to increasing solar activity has also been noted at some altitudes. It is the purpose of this paper to outline these global patterns and to relate them to the physical processes which are now believed to be responsible for their existence. I will not attempt to treat anomalies or detailed behavior, however interesting, but will only discuss those large scale features of the ionospheric temperature patterns which appear to be permanent or reasonably predictable in their occurrence.

Many researchers have contributed to our knowledge of the temperature structure by means of "in situ" probes (Willmore, 1963, Brace et al, 1965, Brace et al 1967, and Donley, 1968). I will not attempt to review all of these,

or the many other measurements which might contribute to a really detailed description of temperature behavior. Instead I will limit my discussion to the data from identical probes on three satellites (Explorer 22, Explorer 32 and Alouette-II) which, when combined, are sufficient to illustrate the major features of the global temperature structure.

The Explorer 22 satellite is especially valuable for latitudinal structure because of its near polar, circular orbit ( $i = 80^\circ$ ,  $1000 \pm 100$  km). Longitudinal structure, though usually small by comparison with other variations, is derived by employing data from the entire network of STADAN telemetry stations (Brace and Reddy, 1965). The diurnal behavior is inferred within any given 3-month period, the time required for  $180^\circ$  precession of the orbit relative to the sun (Brace et al, 1967). Seasonal behavior is evident in the data from consecutive orbital precession cycles and by instantaneous comparisons of the behavior in opposite hemispheres. Finally, solar cycle effects appear in the data from consecutive years (Brace et al, 1968). The long lifetime of this satellite makes it possible to follow the ionospheric behavior from solar minimum in 1964 to solar maximum in 1968-69, although the later results are not yet fully analyzed.

The eccentric orbit of Alouette-II ( $i = 80^\circ$ , 500-3000 km) is highly complementary with that of Explorer 22, because it has the same orbital inclination but traverses a wide altitude range. Similarly, the orbital inclination of Explorer 32 ( $i = 64.5^\circ$ , 280-2700 km) was selected to permit only a slow motion of perigee relative to the orbital precession rate. Therefore, the diurnal variation of the

ionosphere can be observed at many locations without significant distortion due to altitude drift. For this reason Explorer 32 is also complementary with the fixed-altitude Explorer 22. The measurements from all three of these satellites are combined in this paper.

#### THE EXPERIMENTAL METHOD

The observations of  $T_e$  and  $N_e$  reported here have been derived from identical cylindrical electrostatic probes on each of the three satellites. The Explorer 22 probe system is described by Brace and Reddy (1965). Details of the Alouette-II probe system are described by Findlay and Brace (1969), and for Explorer 32 by Brace and Dyson (1969).

Individual point measurements are derived from volt-ampere characteristics in a manner described by Spencer et al, (1965). Briefly, the amplitude of the electron saturation currents provides a measure of  $N_e$  and the shape of the electron retardation region is controlled by the electron energy distribution. If the electrons have a Maxwellian distribution, the retarding region is purely exponential and is represented by the relation,

$$I_e = A N_e e (k T_e / 2\pi m_e)^{1/2} \exp(-eV/k T_e) \quad (1)$$

where

A = probe surface area

e = electron charge

$m_e$  = electron mass

$k$  = Boltzmann's constant

$V$  = potential of probe

Equation (1) becomes

$$T_e = - \frac{e}{k} \frac{dV}{d\ln I_e} \quad (2)$$

The derivative on the right is the measured quantity in the retarding region. A check upon the validity of the measurement is inherent in the analysis because  $dV/d\ln I_e$  must be constant throughout the retarding region which can be resolved over approximately  $5 k T_e$  ( $0 - 5 k T_e$ ).

The amplitude of the current in the electron saturation region is given by:

$$I_e = \frac{AN_e e}{\pi} (2eV/m_e)^{1/2}, \quad \left| \frac{eV}{k T_e} \right| \gg 1 \quad (3)$$

Equation (3) is employed, at positive voltage of about 2 volts, to derive  $N_e$ .

Figure 1 is a theoretical curve, derived from (1) and (3), which identifies the two electron regions of the curve employed to deduce  $T_e$  and  $N_e$ . The ion saturation region, where negligible electron current is collected, serves as the base line from which  $I_e$  is measured.

Figure 2 is a photograph of a section of telemetry record showing two curves from a typical sequence from the Explorer 22 probe. In this case, two curves are taken per second. The current range employed for these curves resolves both the saturation and retardation regions. To provide greater resolution of the

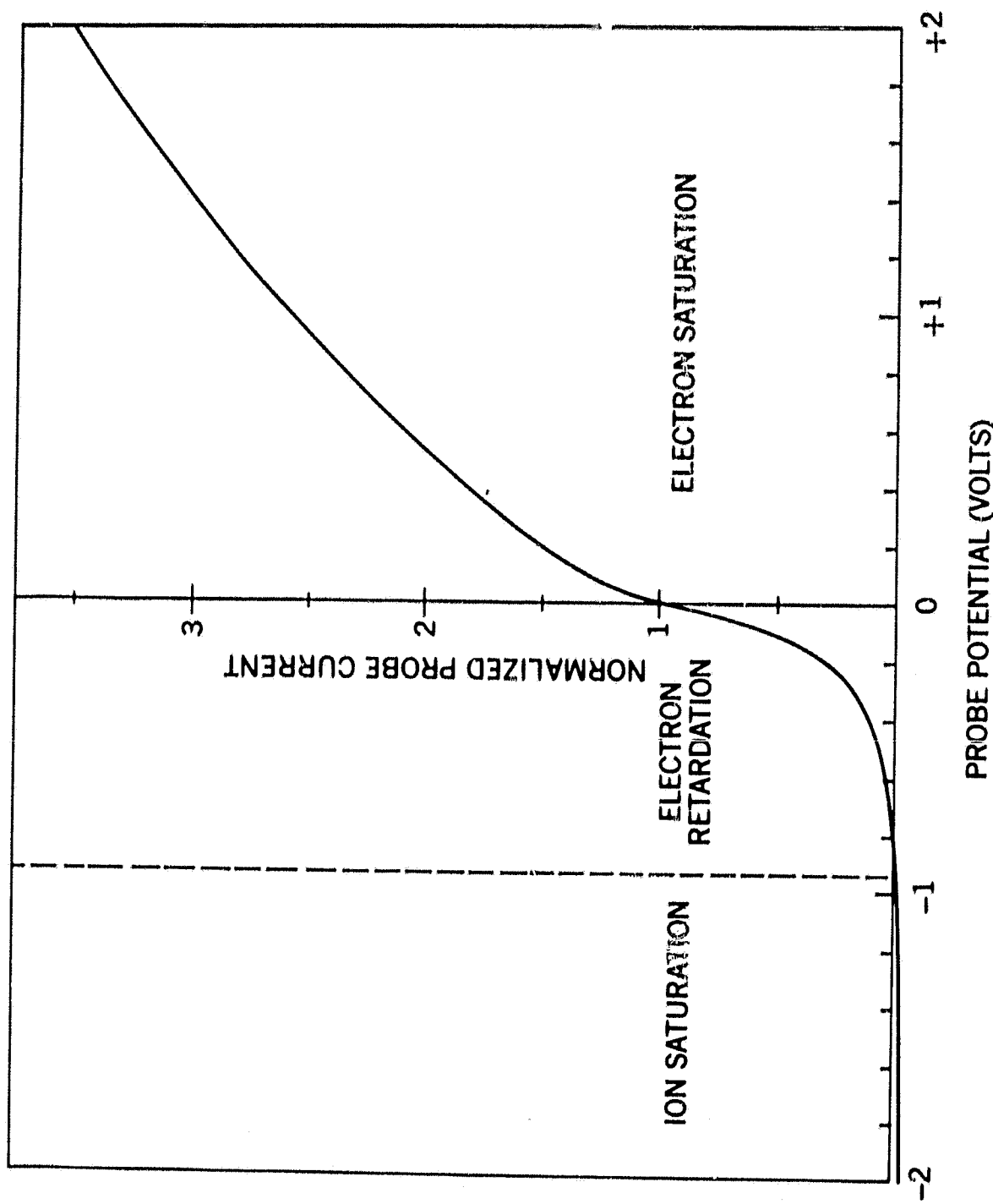


Figure 1—Theoretical voltampere curve. The electron concentration is derived from the amplitude of the curve in the electron saturation region. The temperature is derived from the retardation region. In this region the electron current decreases / a factor of e for each  $kT$  of retarding potential.

**Explorer XXII** Volt-ampere characteristics  
 High  $T_e$   
 High Current Channel

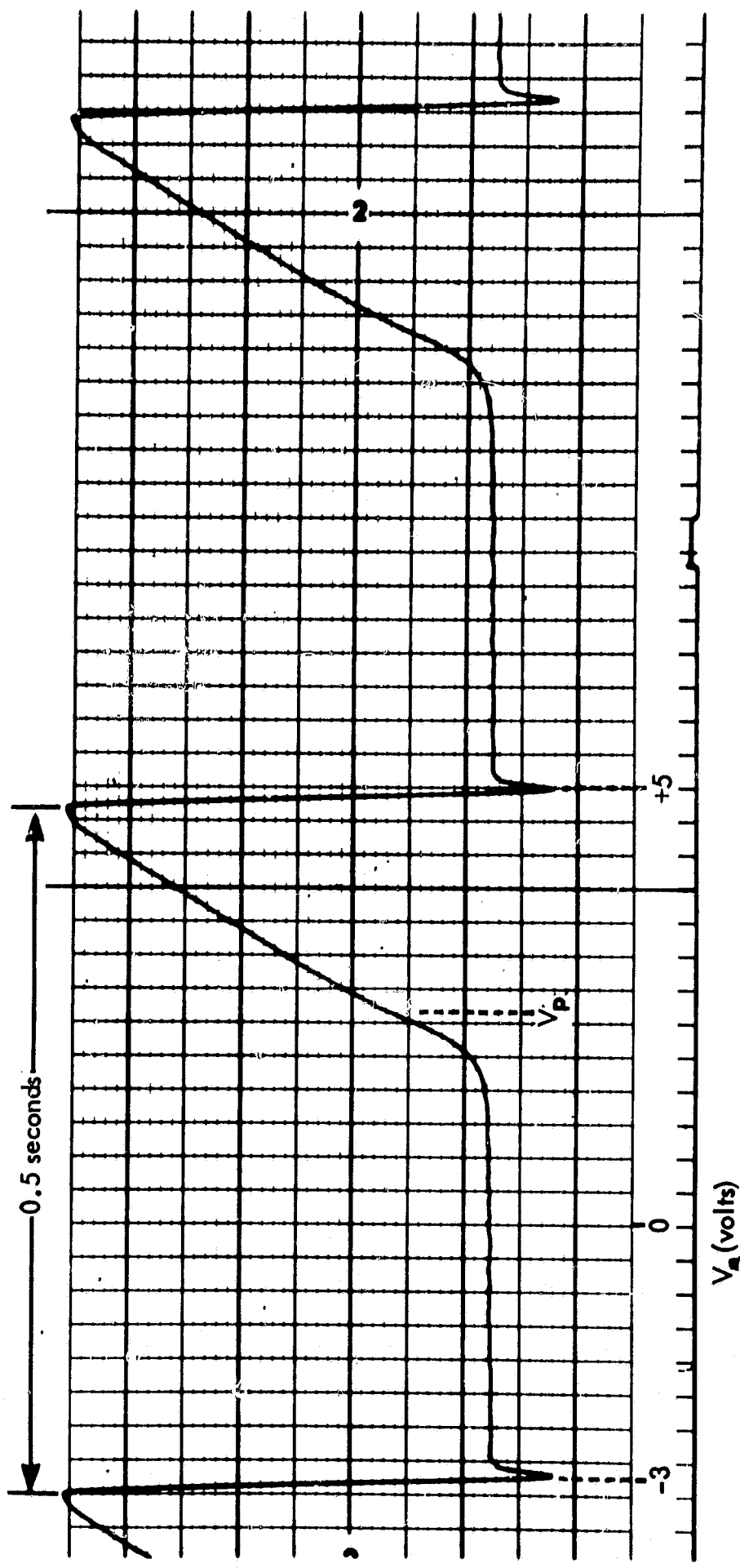


Figure 2—Photograph of section of telemetry record showing a pair of curves from an Explorer 22 sequence. The current range employed here resolves both the electron saturation and retardation regions of the curve.  $V_p$  marks the location of zero potential relative to the plasma.

the retardation region, a more sensitive current range is employed. Figure 3 shows the enhanced resolution which results.

The accuracy of the  $T_e$  measurements varies with the quality of the telemetered signal and the resolution which the current ranges provide. At electron concentrations above  $2 \times 10^3 / \text{cc}$ , the current ranges normally employed introduce less than 5% error in resolution of the retardation region. Additional errors in  $T_e$  introduced by limitations in data quality or choice of data display do not usually exceed 5%.

Errors in  $T_e$  which might be caused by inherent limitations in electrostatic probe theory which may exist would be rather difficult to evaluate, since historically these devices have been employed as laboratory standards to define  $T_e$ . Other methods of determining  $T_e$ , for example microwave measurements, have been evaluated by comparisons with probe measurements.

On the other hand, there has been ample opportunity to compare electron temperatures from various types of direct sensors on the same spacecraft. For example, Donley, et al, (1969) reported excellent agreement among the temperatures from the planar probe, the planar trap and the cylindrical probes on Explorer 31. This agreement is not surprising since all of these probes employ the same basic retarding potential theory which is independent of the collector geometry.

## **Explorer XXII** Volt-ampere characteristics

**High T<sub>c</sub>**      **Low Current Channel**

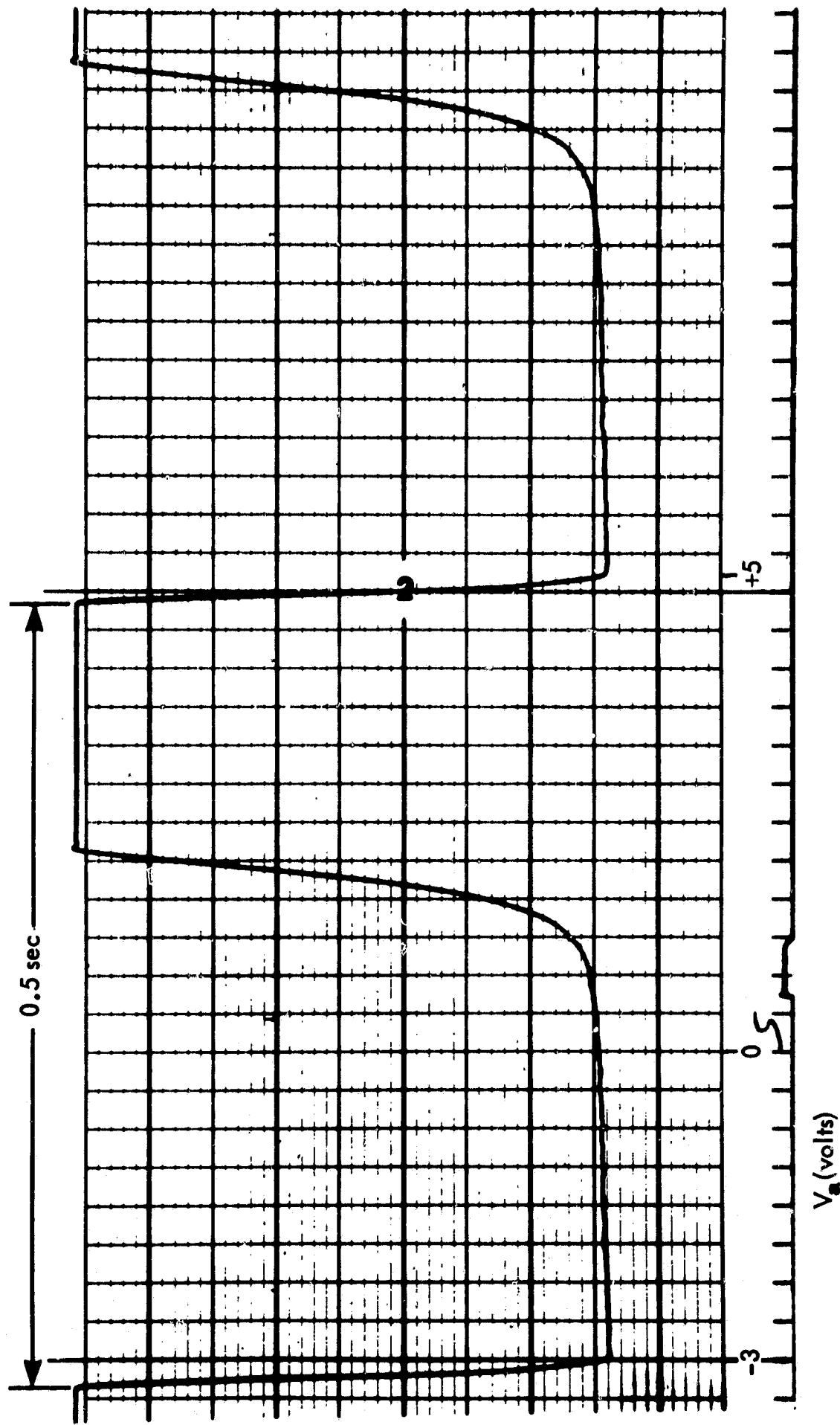


**Figure 3**—Volt-ampere curves taken on a more sensitive current range to enhance the resolution of the retardation region and provide greater accuracy in  $T_e$ .

## THE OBSERVATIONS

### Pole-to-Pole Plots (1000 km)

When point-by-point measurements about the orbit are combined, many of the major features of the ionosphere are evident without further analysis. For example figure 4a shows computer plots of the Explorer 22 data taken in a single week of May 1965, and 4b shows data from another week in November 1965. These periods are approximately one orbital precession cycle apart so that the local time patterns, seen on the bottom frame, are the same. In both of these periods the major dayside and nightside features are readily observed. The dayside  $T_e$  is characterized by generally high values at middle latitudes ( $\approx 3000^{\circ}\text{K}$ ), and an equatorial depression by about 30%. The corresponding dayside  $N_e$  structure behaves inversely with  $T_e$ , except toward high latitudes where both  $N_e$  and  $T_e$  decrease.

The nightside  $T_e$  exhibits a broader equatorial trough, with  $T_e$  increasing rapidly between  $30^{\circ}$  and  $60^{\circ}$  geomagnetic latitude. The value of  $T_e$  in the nightside trough is not constant, but exhibits significant differences between these two periods (May and November, 1965) and important variations within each of these one week periods. The detailed nature of these nightside variations at low latitudes has not been examined thoroughly enough to suggest a heat source for them, however these variations are clearly present. For example figure 5 shows the data from a week in January of 1967. The equatorial temperature is about  $1200^{\circ}\text{K}$ . A strong minimum in  $T_e$  exists at  $20^{\circ}$  to  $30^{\circ}$  South at American

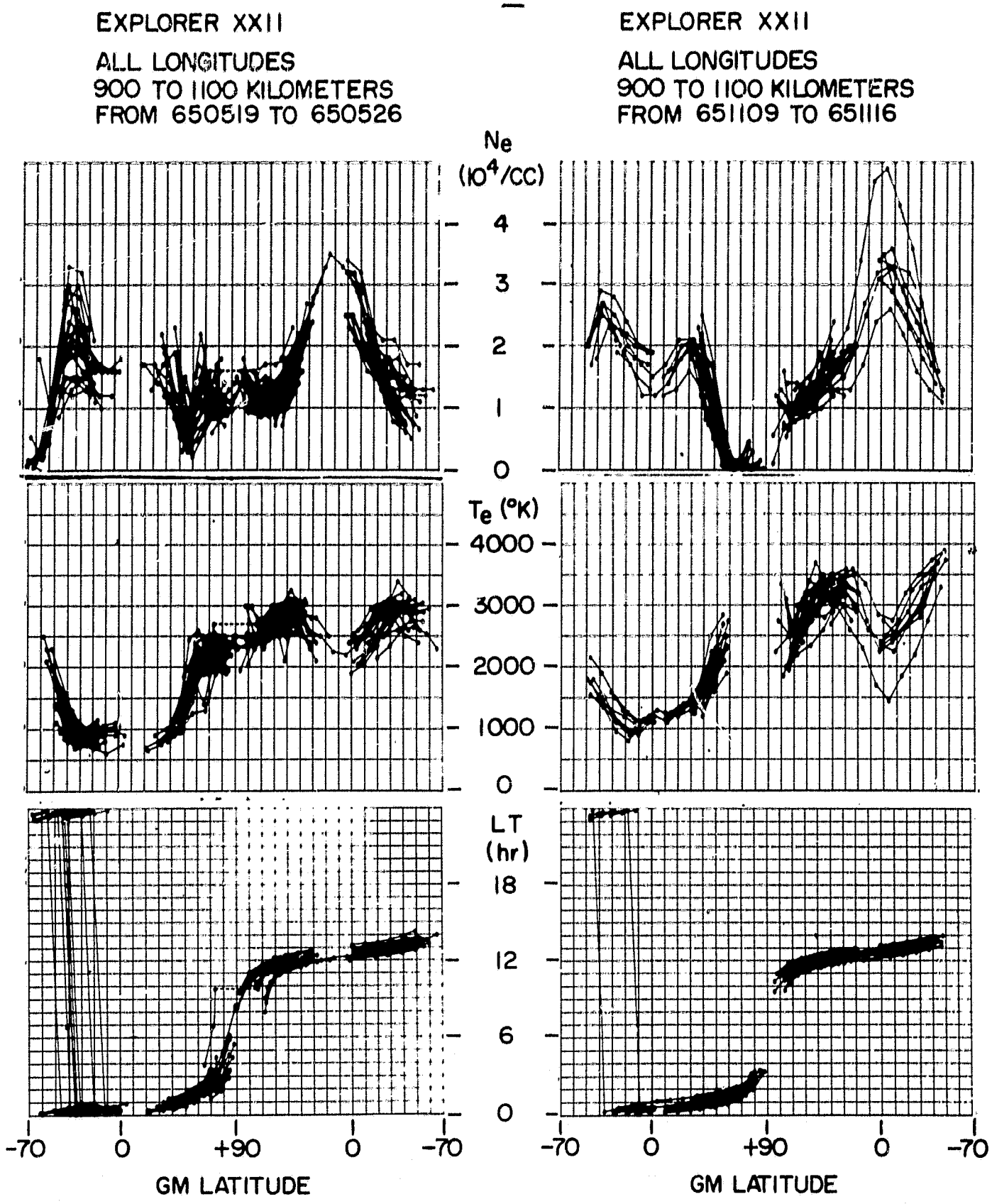


Figure 4a—A pole-to-pole computer plot of a week of measurements (May 19-26) in summer of 1965.

Figure 4b—A pole-to-pole computer plot of a week of data (Nov. 9-16) in winter of 1965.

EXPLORER XXII

ALL LONGITUDES  
900 TO 1100 KILOMETERS  
FROM 670117 TO 670124

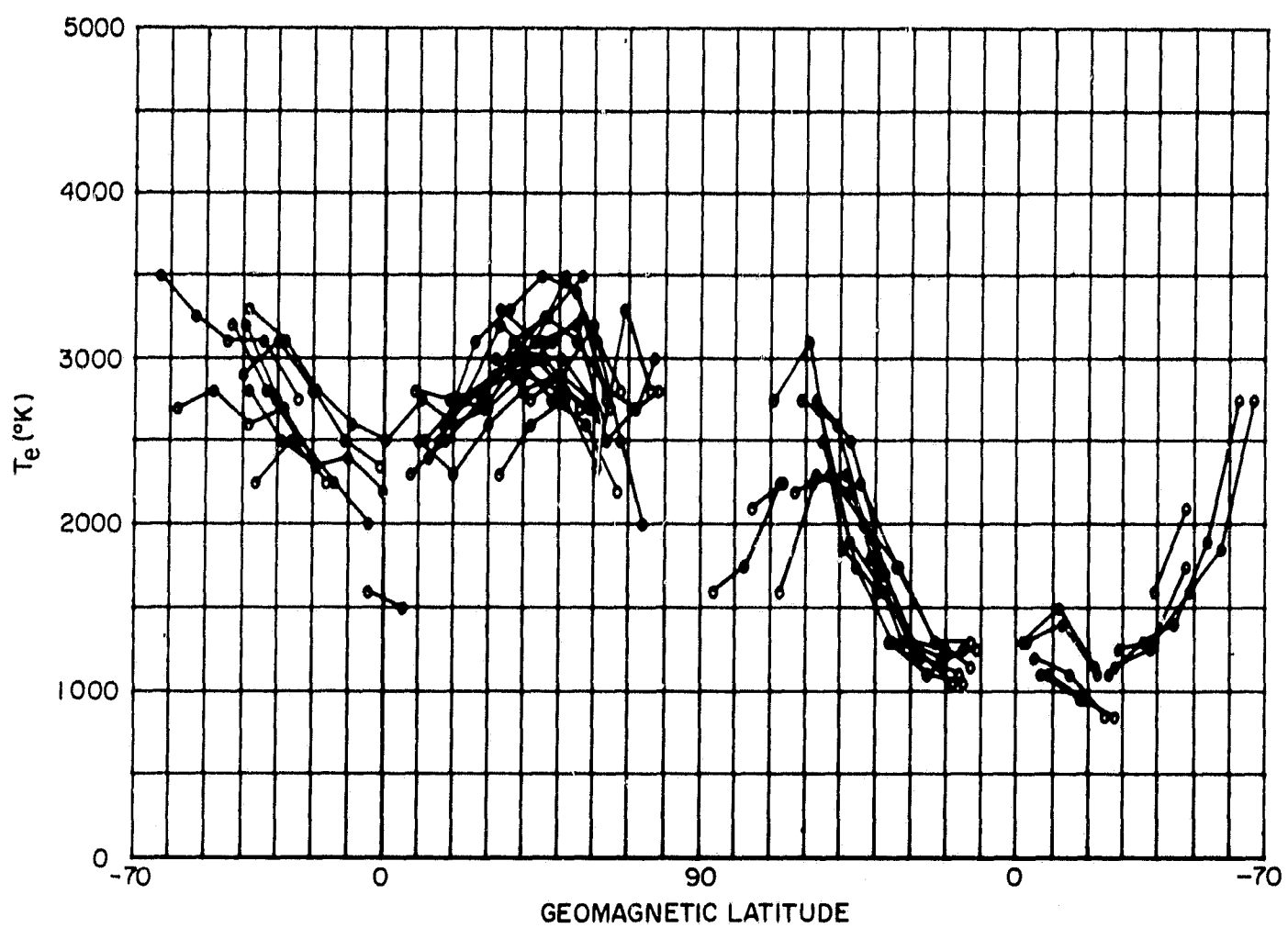


Figure 5-A pole-to-pole computer plot showing detailed structure of  $T_e$  within the equatorial nighttime trough.

longitudes where  $T_e \approx 1000^\circ\text{K}$ . This minimum is greatly diminished, or non-existent at European and Australian longitudes. This strong localized minimum has been a consistent feature of the nightside ionosphere since late 1965, and was already well developed in November 1965 (see figure 4b).

#### Local Time Behavior (1000 km)

As the orbital plane precesses relative to the sun, the plots from consecutive weeks display the corresponding diurnal changes in the ionosphere. For example, the diurnal variation of  $T_e$  and  $N_e$  near vernal equinox of 1965 are summarized in figures 6 and 7. These figures have been discussed by Brace et al (1967). The major temporal behavior to note is the rather large diurnal variation in  $T_e$  at low latitudes and the smaller variation at middle and high latitudes.

#### Solar Cycle Variations (1000 km)

Both the daytime and nighttime temperatures increase with solar activity by a factor which is much greater than the expected increase in neutral gas temperature (Jacchia, 1964). This is evident in figure 8 which shows the latitudinal structure of  $T_e$  and  $N_e$  at one year intervals in 1965, 1966 and 1967 (Brace, et al, 1968). The equatorial nighttime temperature increased by about  $300^\circ\text{K}$  between 1965 and 1966, and the daytime temperature increased by about  $1000^\circ\text{K}$  at all latitudes in this period. The daytime  $T_e$  had decreased significantly by 1967 but the nighttime values changed little.

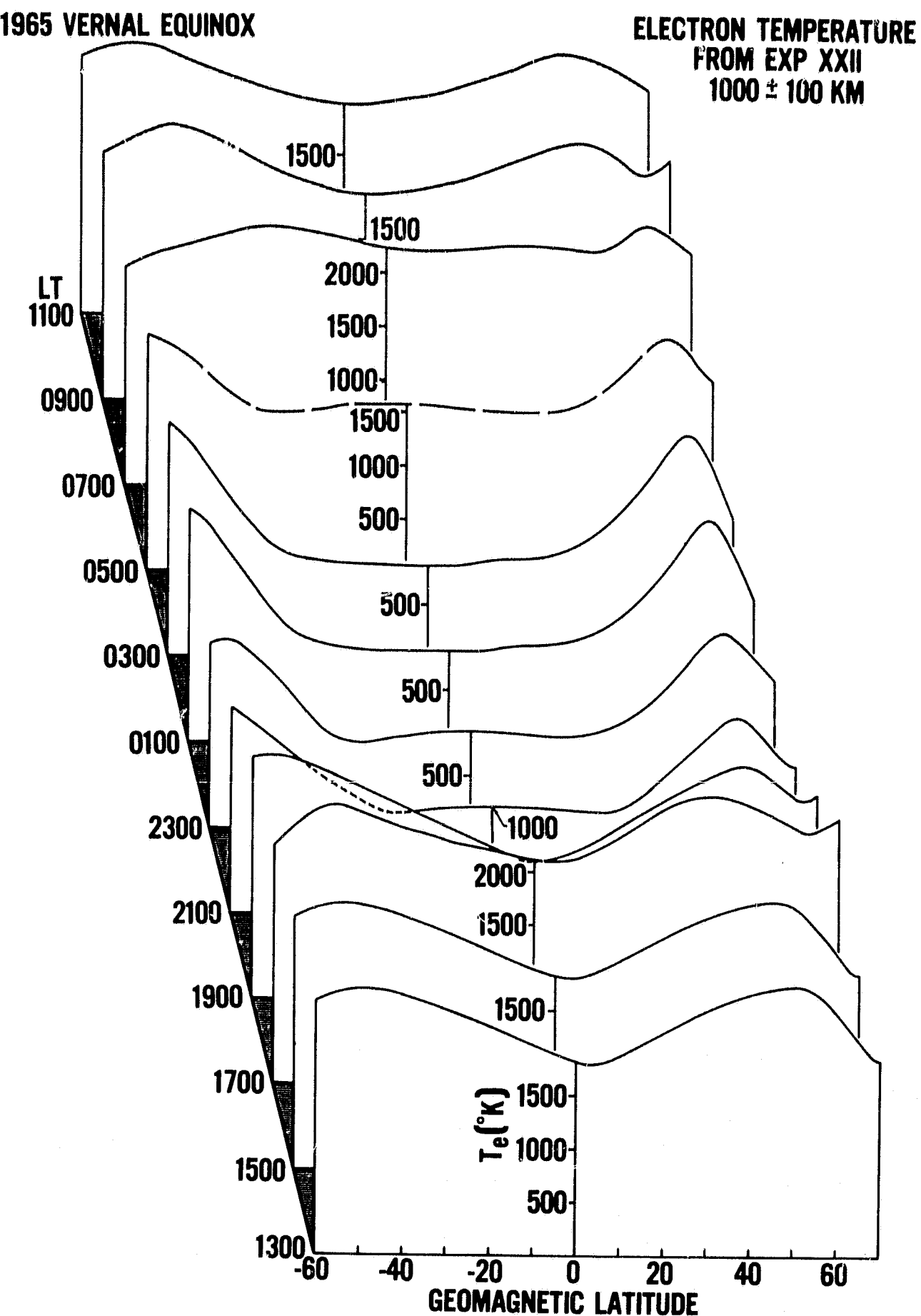


Figure 6—Local time behavior of  $T_e$  near vernal equinox, 1965.

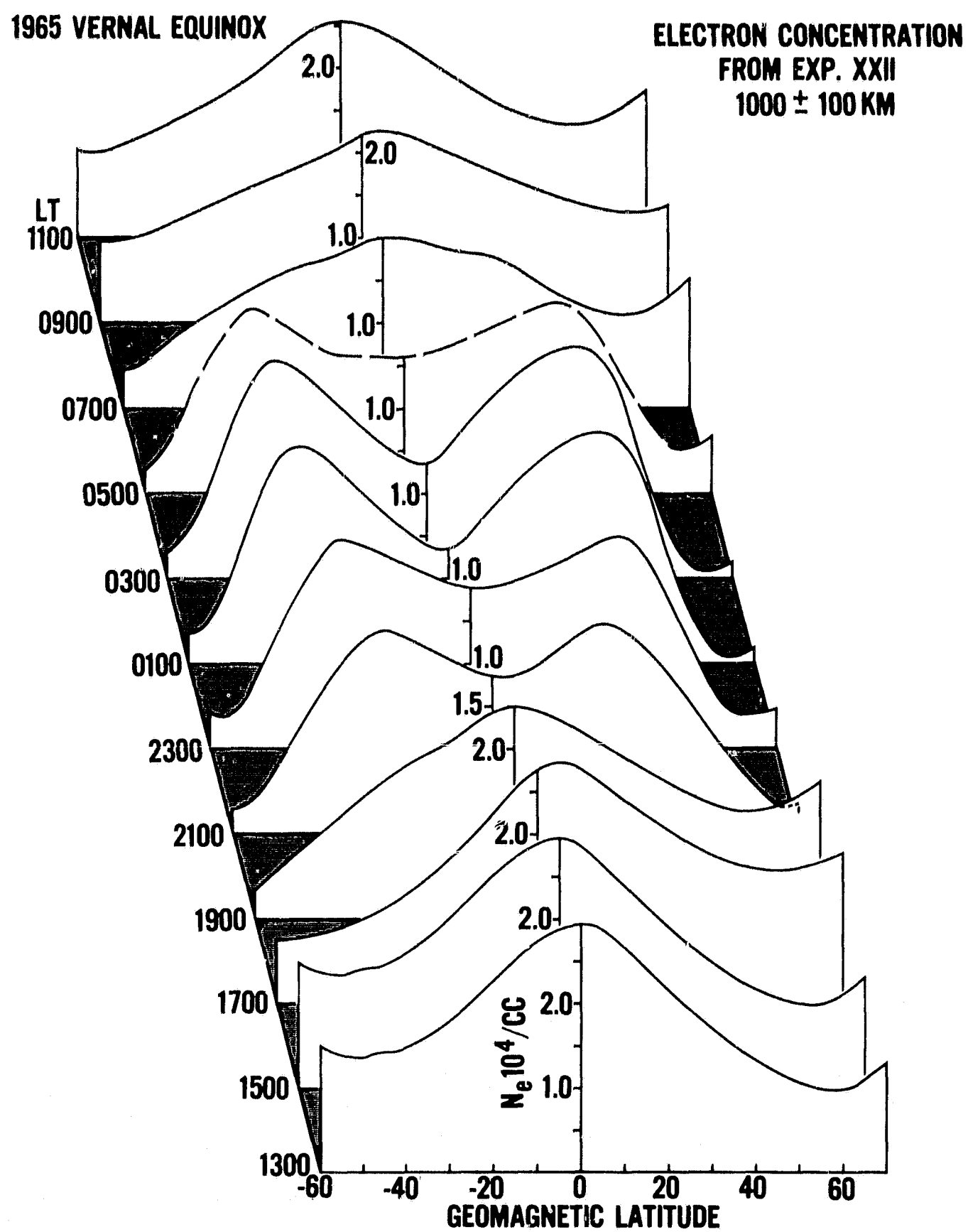


Figure 7—Local time behavior of  $N_e$  from same orbits as figure 6.

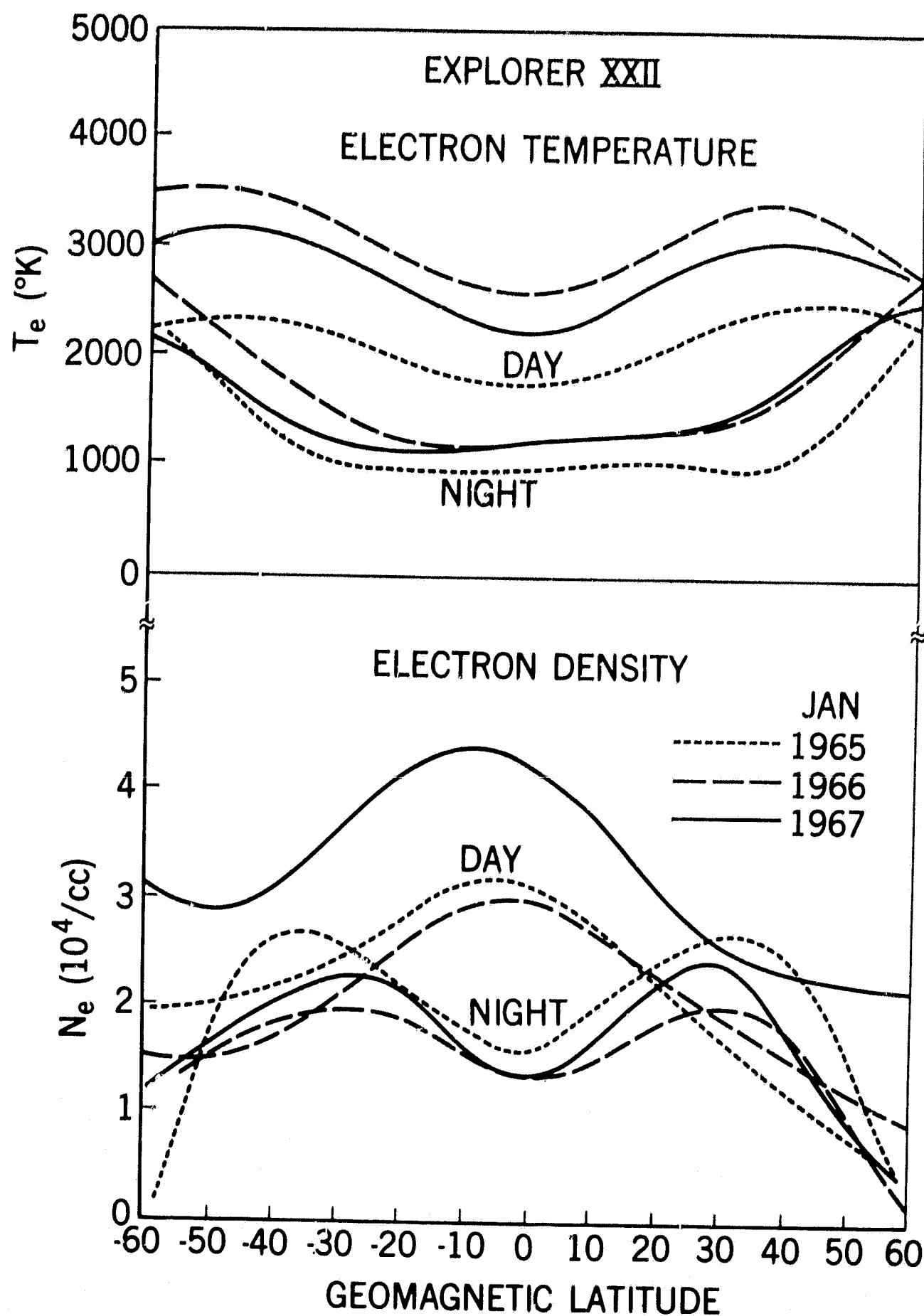


Figure 8—Latitudinal structure in three consecutive years.

### Polar Ionosphere at Solar Minimum (1000 km)

Figure 9 illustrates the daily polar coverage often available from Explorer 22. The lines represent the subsatellite path where measurements were obtained on the day of December 20, 1964. As the Earth rotated under the orbit, European, American and Pacific longitudes were traversed sequentially by both the northbound and southbound halves of the orbit. The northbound half was on the nightside ( $\approx$  2200 hours) and the southbound half was on the dayside ( $\approx$  0900 hours), however the entire polar cap was dark on this date. One should keep in mind that the orbit can be viewed as fixed relative to the sun vector over periods as brief as a few days. Therefore, as the Earth rotates, the only variations observed from orbit to orbit are those induced by longitudinal structure in the ionosphere. Any short-term variations which may occur, such as magnetic storms, can usually be recognized by their deviations from the mean behavior over a several day period.

### Winter Polar Ionosphere

To illustrate the polar ionosphere structure on one day, in figure 10 we have combined the measurements taken during the passes shown in figure 9. Many of the winter pole characteristics are evident. A trough of low  $N_e$  over the entire polar cap is apparent in the passes at all longitudes, a phenomenon which has been well documented (Hagg, 1968).  $T_e$  also exhibits a significant trough over the pole, although the density was often too low to permit accurate

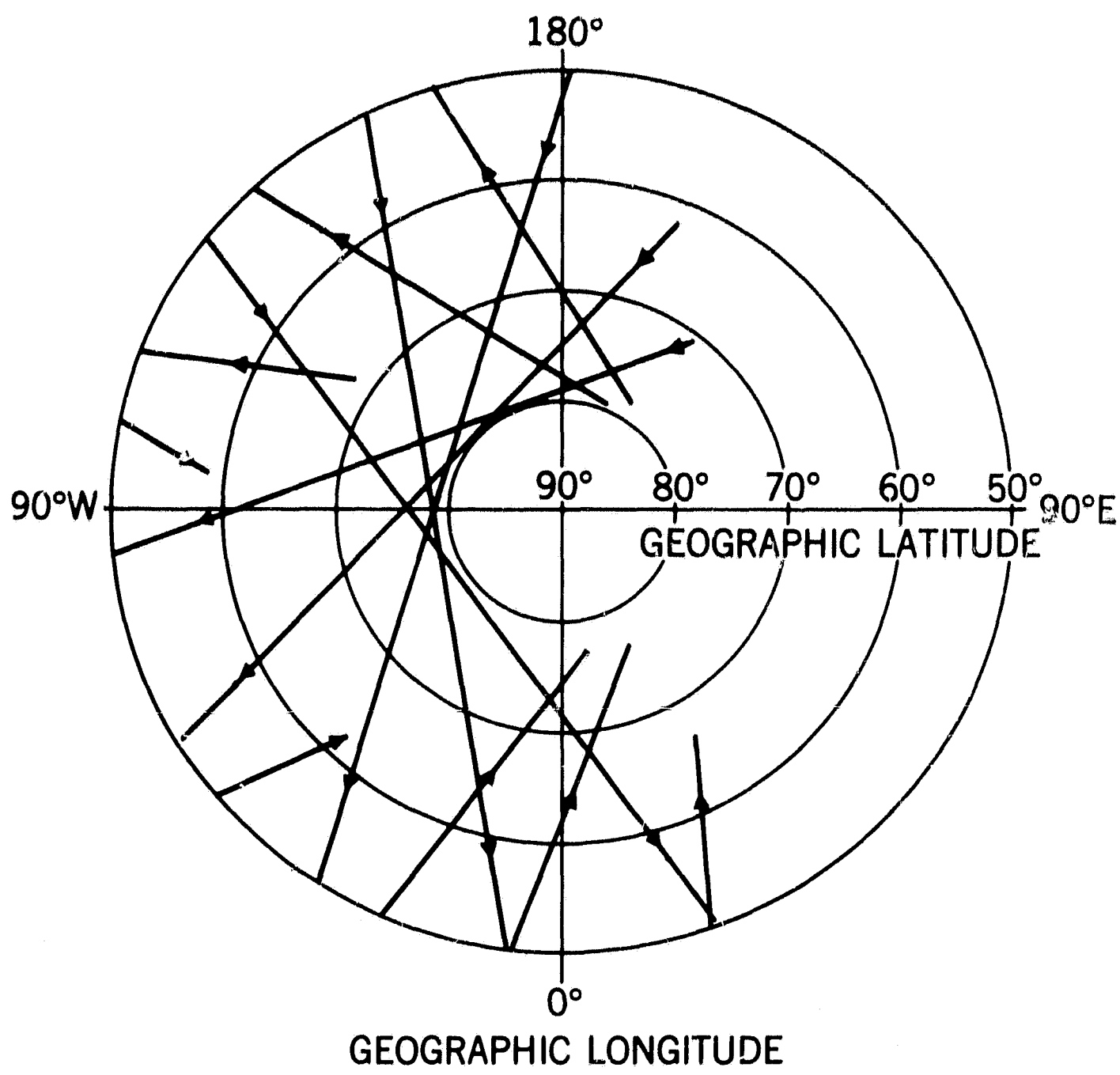


Figure 9—Polar coverage on Dec. 20, 1964. Arrows indicate the direction of satellite motion.

EXPLORER XXXI DEC. 20, 1964

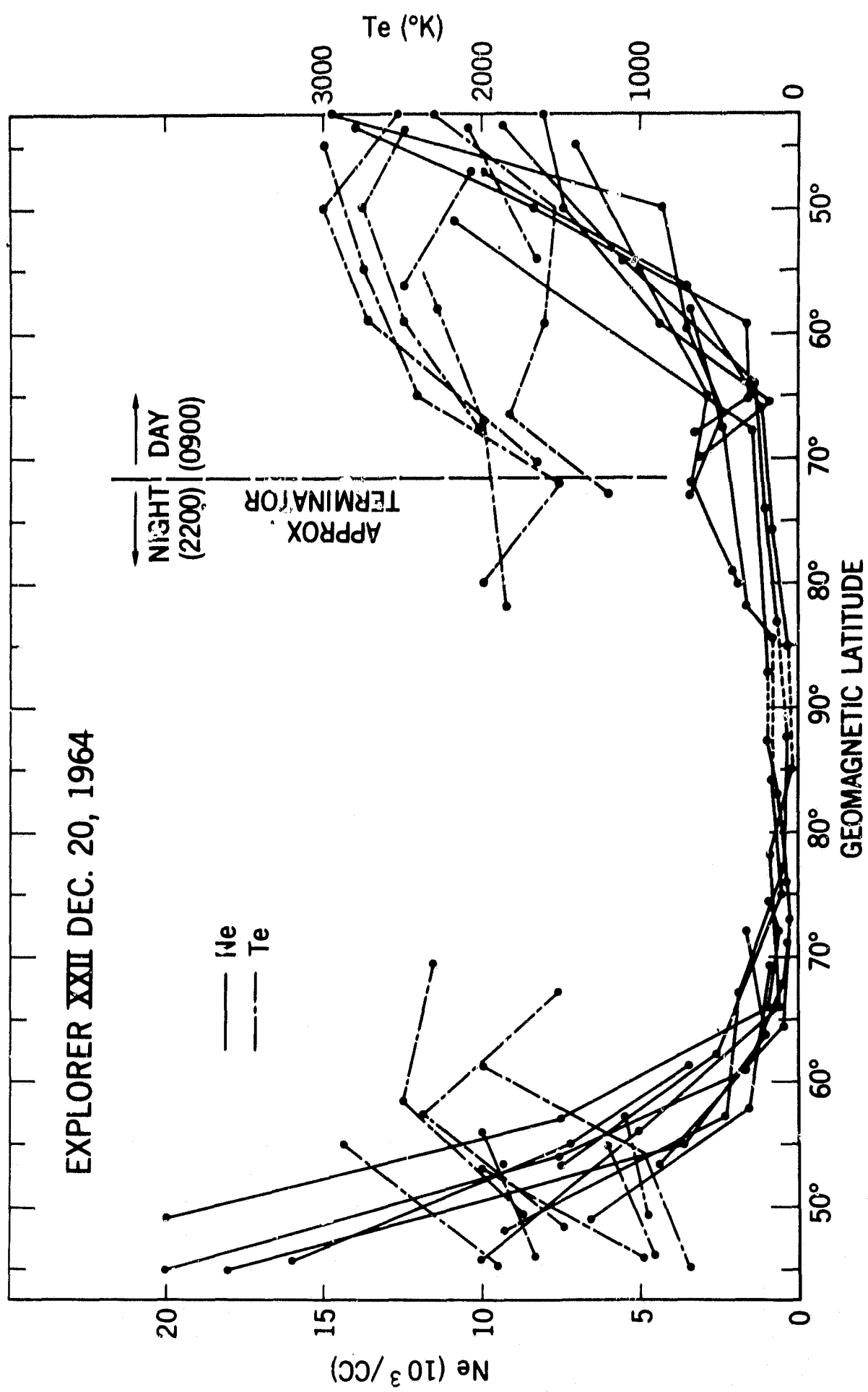


Figure 10— $T_e$  and  $N_e$  measured during polar the passes shown in figure 9. The approximate position of the solar terminator at 300 km is indicated. The deep trough in  $N_e$  is characteristic of the winter pole. A polar trough in  $T_e$  is also evident, but  $N_e$  was often too low to permit  $T_e$  to be resolved accurately.

$T_e$  resolution over much of the polar cap. The peak in  $T_e$  near  $60^\circ$  on the nightside boundary of the polar cap is a consistent feature reported earlier by Brace and Reddy (1965). This enhanced  $T_e$  is probably produced by heat conduction downward from the protonosphere. The higher values of  $T_e$  on the dayside of the trough probably reflect both solar heating and heat conduction from above.

When data from several consecutive days are combined, a significant degree of longitudinal resolution results and a global pattern emerges. Figure 11 shows this pattern, in the form of contour plots, for the night half of the polar cap (up to the magnetic pole) during the period Dec. 25-29, 1964. From this pattern it can be seen that the  $T_e$  and  $N_e$  trough over the pole occurs at all longitudes which are in range of the STADAN ground stations. The nightside peak of  $T_e$  near  $60^\circ$  can be identified at all longitudes but is clearly enhanced at American longitudes.

#### Summer Polar Ionosphere

Data from a similar series of passes over the polar cap in summer are shown in Figure 12, and contours from a several-day period are shown in Figures 13 and 14. It is not surprising that  $T_e$  and  $N_e$  are higher over the summer pole. However, in spite of the increased  $T_e$  within the polar region, the trough of  $T_e$  does not entirely disappear in summer. The  $T_e$  peak at  $60^\circ$  which forms the nightside boundary of the polar trough is not as high in summer, a fact that has been noted by Evans (1967) from radar backscatter measurements near that latitude.

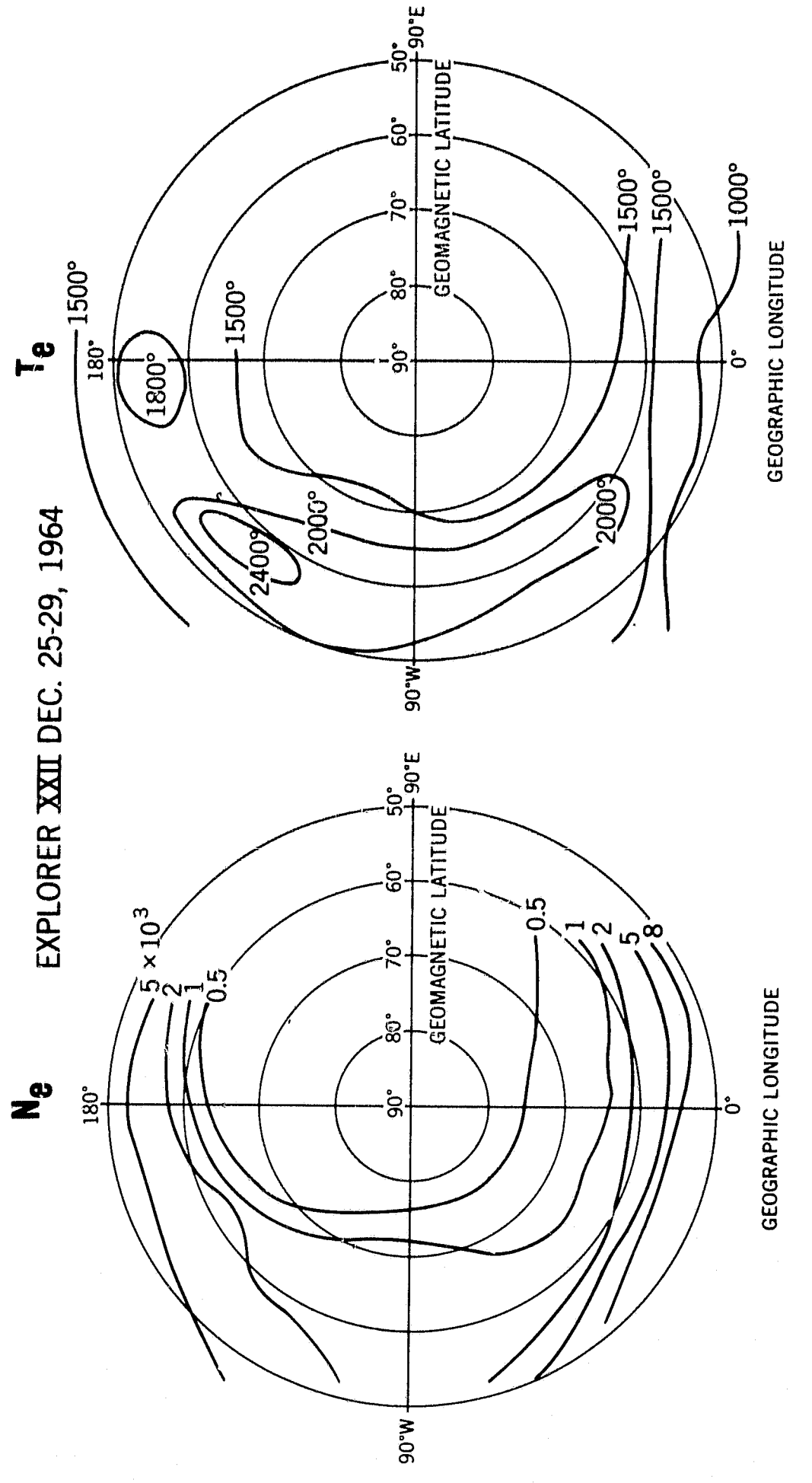


Figure 11—Contour plots of  $T_e$  and  $N_e$  over the nightside of the winter pole showing the longitudinal structure.

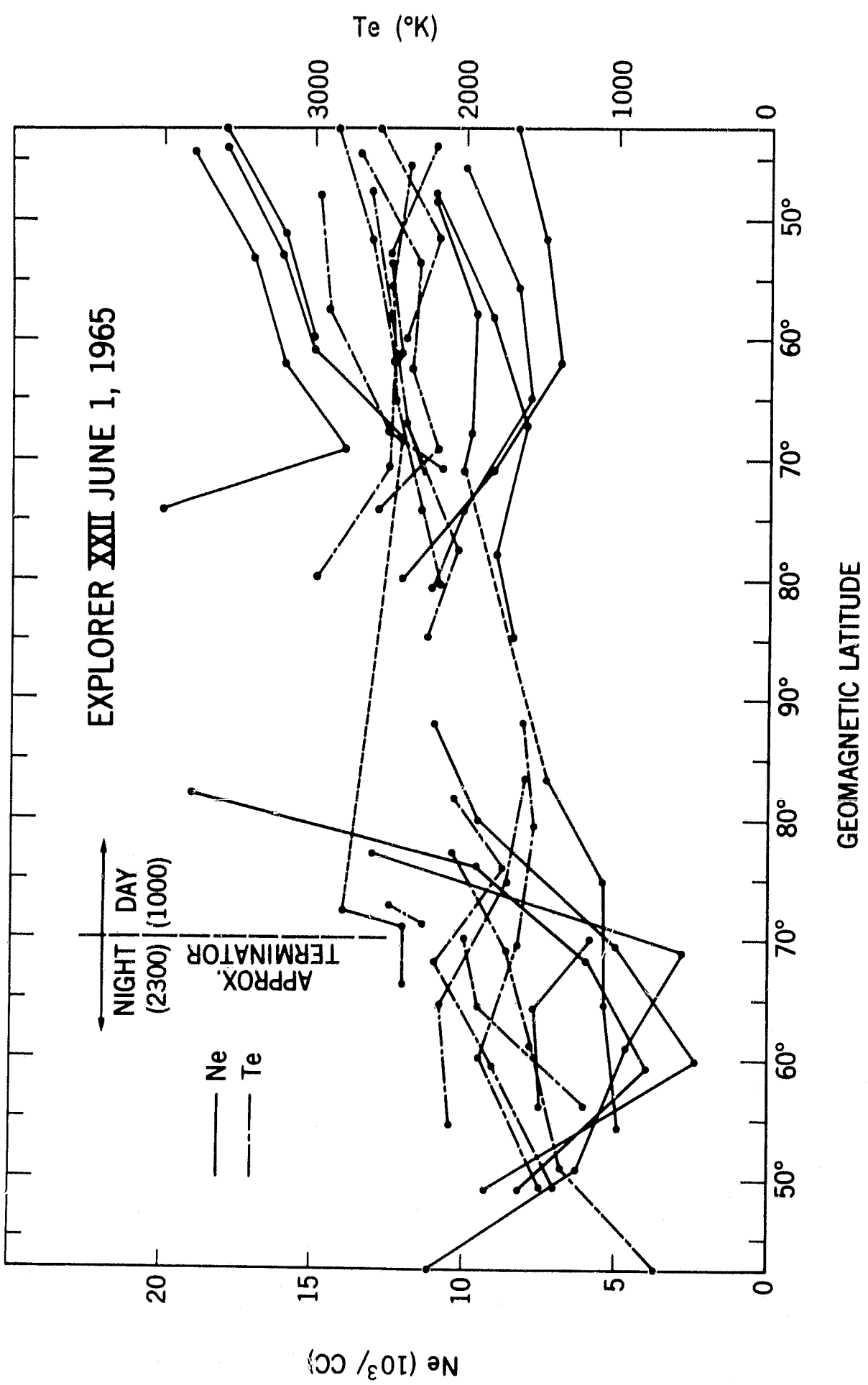


Figure 12— $T_e$  and  $N_e$  measured during passes over the pole in summer on June 1, 1965.

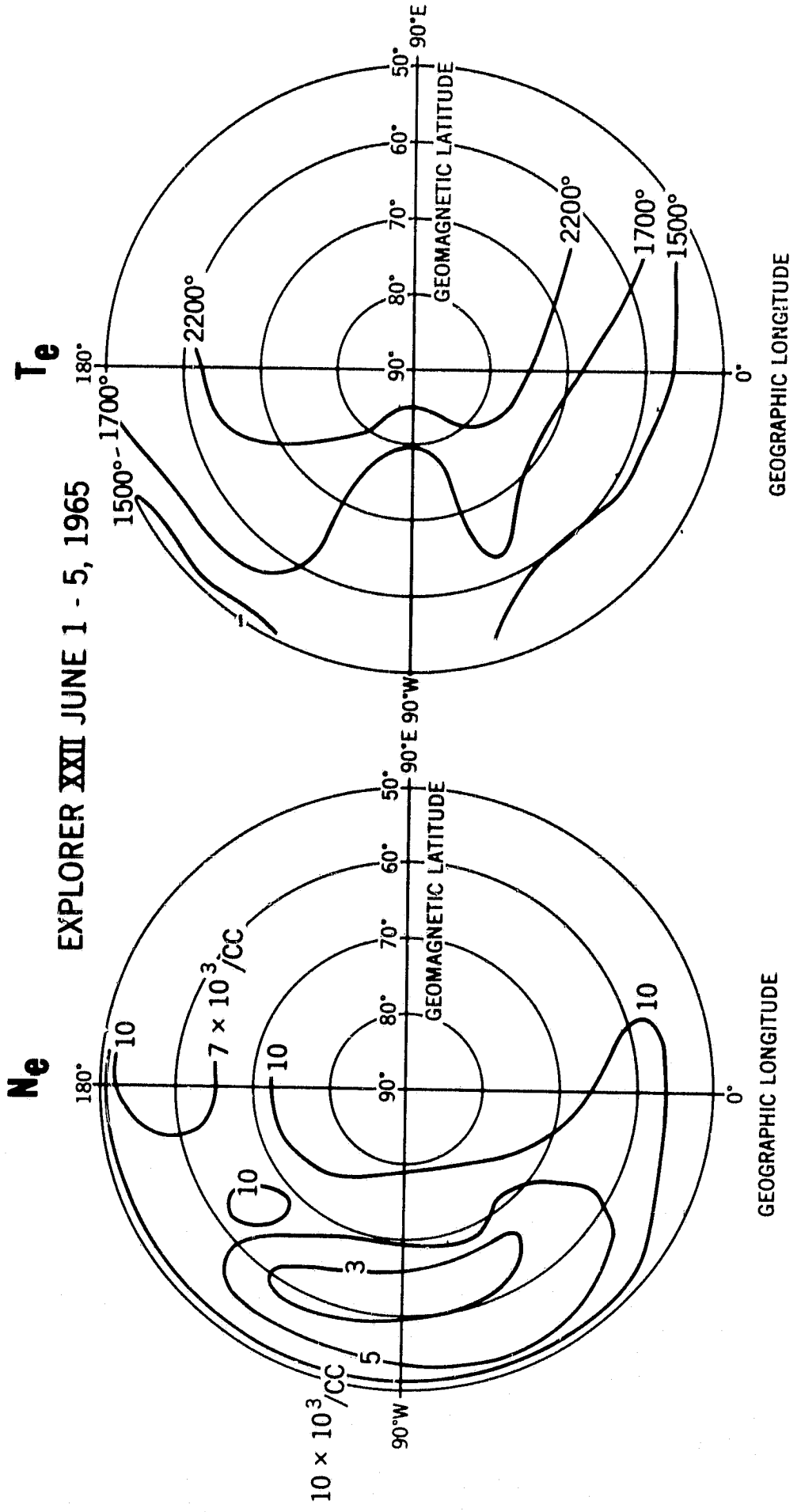


Figure 13—Contour plots of  $T_e$  and  $N_e$  over the nightside of the summer pole showing longitudinal structure.

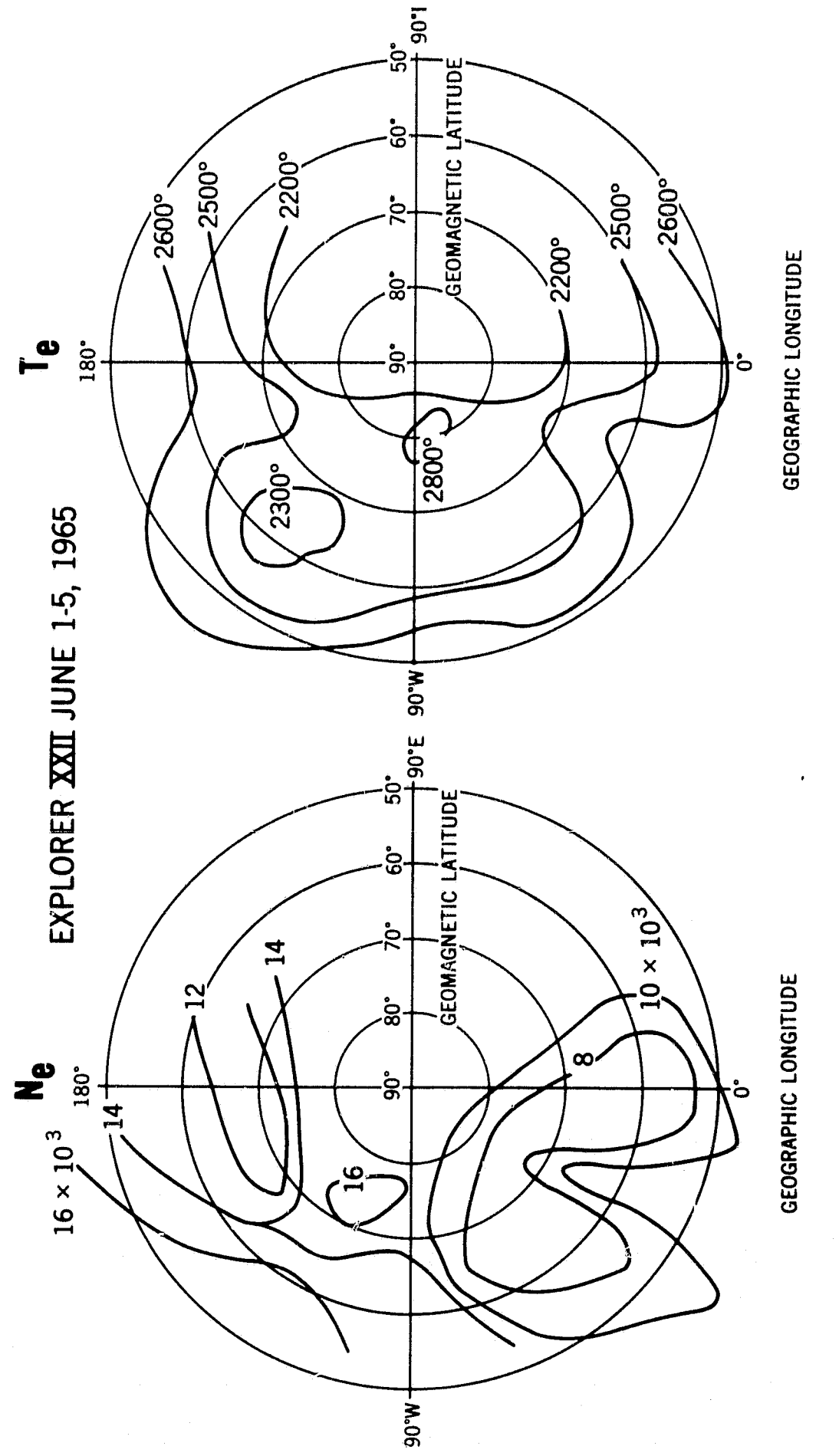


Figure 14—Contour plots of  $T_e$  and  $N_e$  over the dayside of the pole in summer.

Several well known  $N_e$  features are evident in the nightside contours of Figure 13. The "main trough" in  $f_0 F_2$ , found by Muldrew (1965) at American longitudes, is also present in the contours at 1000 kilometers. This trough, which is centered between  $60^\circ$  and  $65^\circ$  geomagnetic latitude, is especially deep at American longitudes but can still be identified at European and Pacific longitudes. Its extraordinary depth at American longitudes may be a simple solar zenith angle effect. Perhaps the depletion mechanism that produces the trough is operating at all longitudes, but the tilt of the Earth's magnetic pole toward American longitudes permits only American portions of the trough region to remain in darkness long enough for a trough to develop fully. At European and Pacific longitudes, the trough region at 300 kilometers is illuminated all night at summer solstice.

The dayside contours over the summer pole, shown in figure 14, exhibit consistent features in  $T_e$  and  $N_e$  which have not yet been interpreted. The shallow polar trough of  $T_e$ , pointed out earlier, is the main prevailing feature.

In summary, the electron temperature in the polar ionosphere exhibits smaller temporal variations than are observed at low latitudes. The summer temperature is not as great as those found in the daytime at middle latitudes where heat conduction from the protonosphere is an important source of F-region heating. Conversely, the polar winter temperatures are somewhat greater than those found at night at the equator. This implies that an even larger nocturnal heat source may be at work within the polar cap, than is

present in the equatorial region at night. The feasibility of such a source is rather easy to accept in view of the close coupling between the polar ionosphere and potential sources of energy in the magnetosphere.

#### Diurnal Variation of Protonosphere Temperature (1000-3000 km)

The apogee data from Explorer 32 provide a detailed view of the diurnal variation in protonosphere electron temperature at moderate solar activity. Figure 15 shows the variation in  $T_e$  and  $N_e$  encountered above the equator at an altitude of about 2600 kilometers ( $L = 1.4$ ). In the seven-month period between July 1966 and February 1967, the orbit precessed through about 44 hours of local time. Although the  $T_e$  variations repeat quite well from one precession cycle to the next, the values of  $N_e$  increased steadily throughout this period and exhibited increasing amounts of day-to-day variability. It is likely that both of these effects occur in response to the increasing level of solar activity.

A major seasonal effect is evident in the longer duration of the "night" at equinox (August-September data). At this time the F-region at both ends of the  $L = 1.4$  field tube remain dark for almost 10 hours. Therefore at equinox this field tube is free from photoelectron heating for the longest possible time. At solstice, however, the summer end of this tube is dark for only 6 hours and the temperature on this tube remains low only during this period.

To examine the altitudinal behavior of  $T_e$  along this tube, Brace and Mahajan (1969) have combined the Explorer 32 data from figure 15 with Explorer 22 data taken in the same period at the 1000 kilometer foot of this field line. These

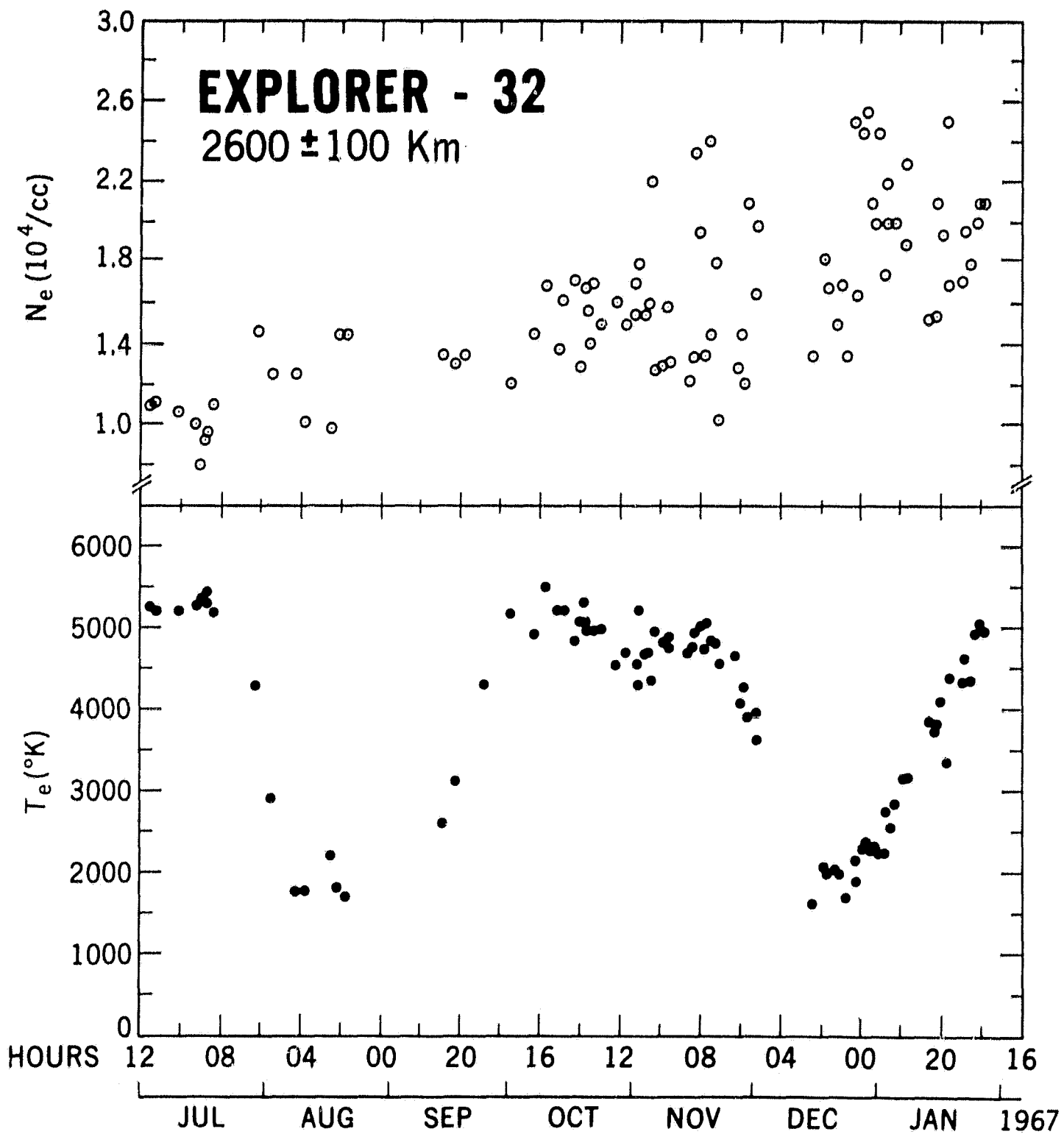


Figure 15—Equatorial measurement of  $T_e$  and  $N_e$  at 2600 km from Explorer 32, taken as the orbit precessed through 44 hours of local time.

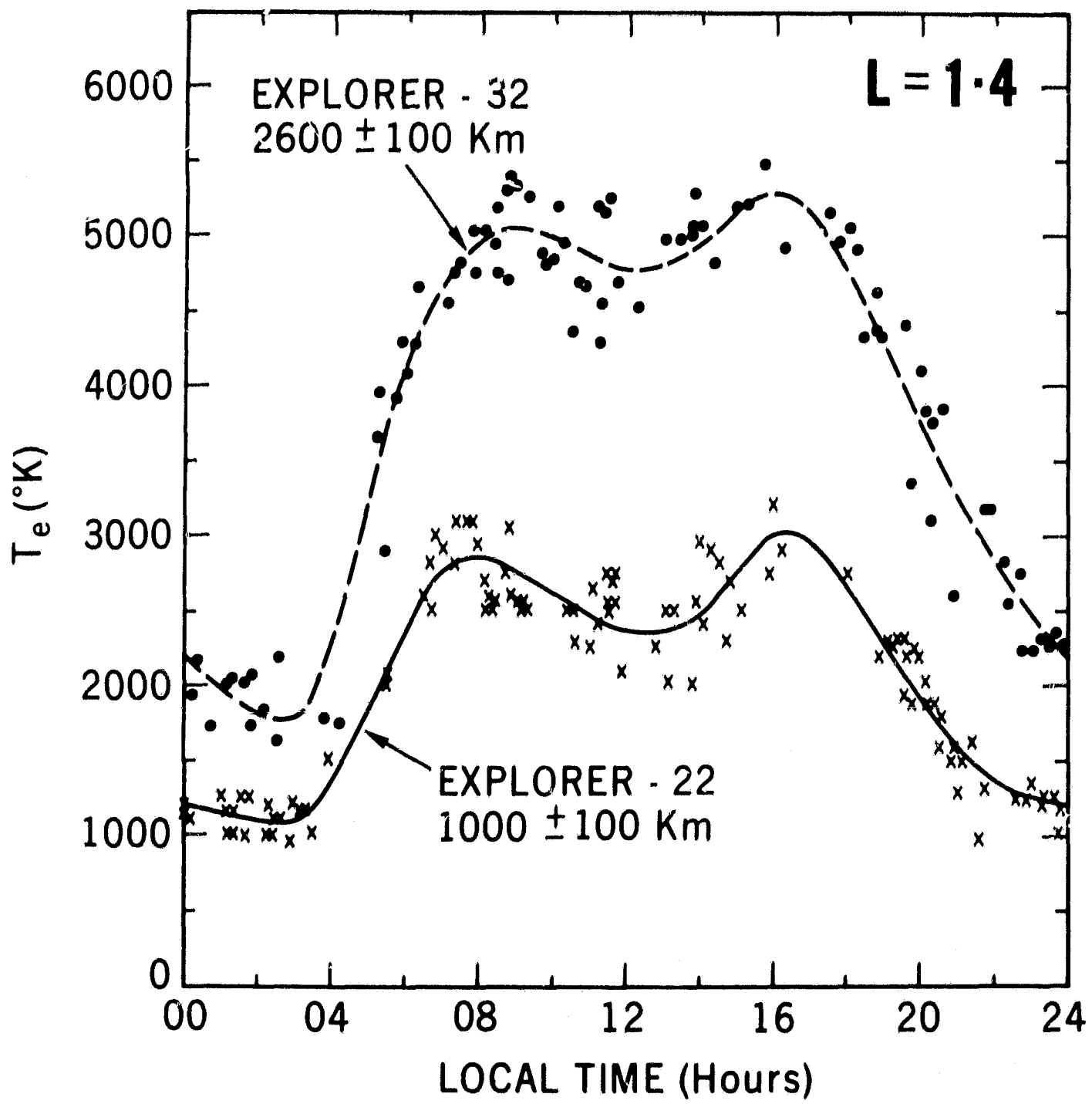


Figure 16—Combined  $T_e$  measurements from Explorer 32 and 22 show the diurnal variation at two altitudes along a single field tube  $L = 1.4$ . The difference in temperature at these two altitudes reflects the temperature gradient along this tube.

combined  $T_e$  measurements are shown in figure 16. The difference in  $T_e$  at these two levels represents the diurnal variation in the temperature gradient along this field tube.

#### Latitude Structure of $T_e$ in the Nightside Protonosphere

By combining measurements from Explorer 22 and Alouette-II when their orbital planes were nearly parallel, Mahajan and Brace (1969) have compared latitudinal structure at 1000 and 2500 km. Figure 17 shows the mean nighttime temperatures found at these two altitudes in the summer of 1966. From the difference between these profiles the temperature gradient along field lines between  $35^\circ$  and  $60^\circ$  was derived. At  $35^\circ$  ( $L = 1.4$ ), the lowest field time which reaches 2500 km, the temperature gradient varied from about  $0.5^\circ/\text{km}$  at 1000 km to about  $0.25^\circ/\text{km}$  at 2000 km. The gradient increased with latitude reaching as high as  $2^\circ/\text{km}$  at 1000 km on the  $60^\circ$  field line ( $L = 4$ ). These authors concluded that the observed temperatures could be maintained throughout the night by the normal heat capacity of the protonosphere without invoking any additional heating mechanism. Nagy et al (1968) arrived at similar conclusions on theoretical grounds.

#### DISCUSSION

##### Processes Controlling the Electron Temperature

The global distribution of  $T_e$  and its temporal behavior represents the changing balance between the processes which heat and cool the electrons (Mayr et al, 1967). In those portions of the atmosphere which are illuminated

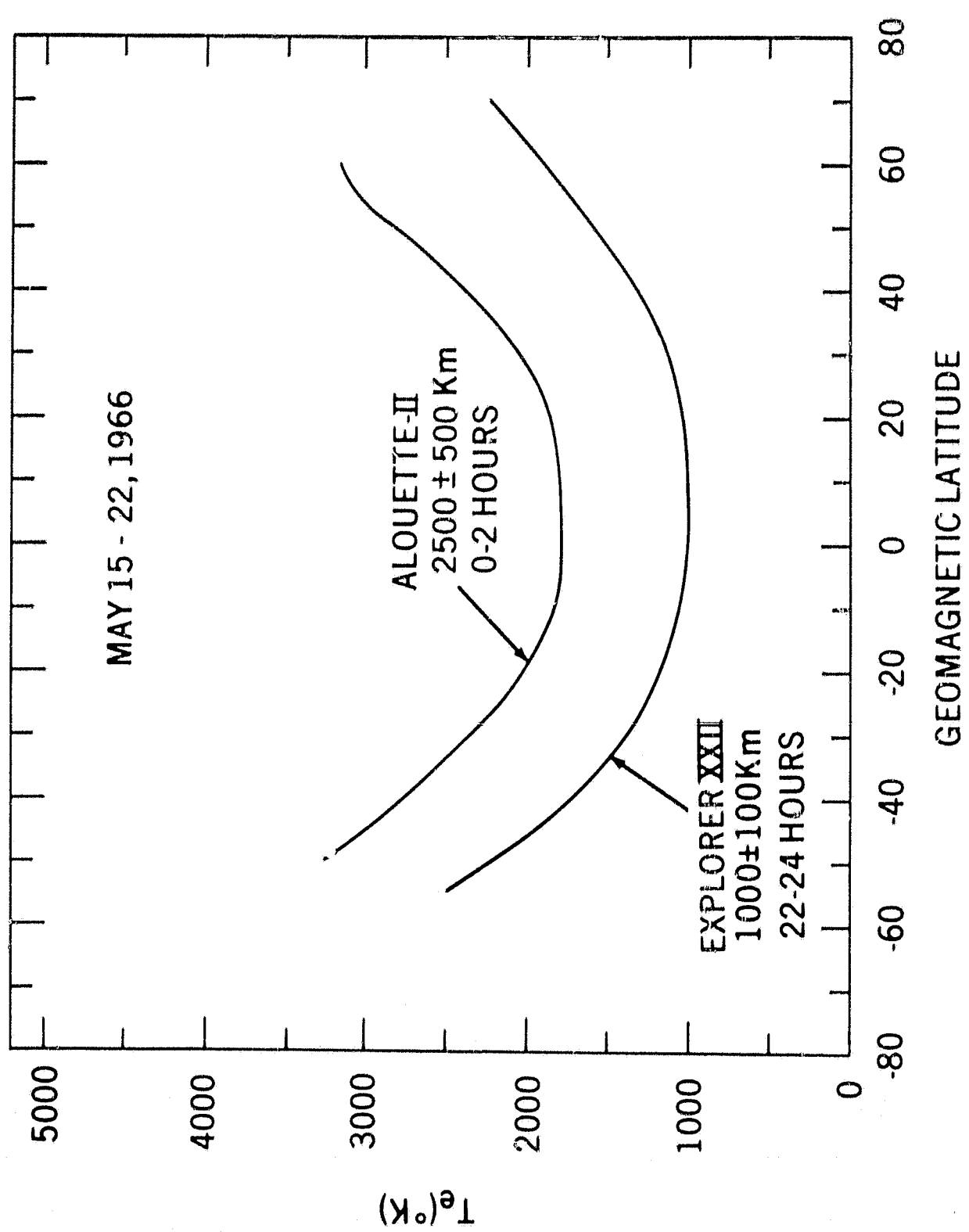


Figure 17—Combined  $T_e$  measurements from Explorer 22 and Alouette-II show the latitudinal variation at two altitudes. The difference in temperature at these two altitudes reflects the latitudinal variation in the temperature gradient.

by the sun, thermal electrons are heated by collisions with photoelectrons recently produced by photoionization of the neutral constituents (Hanson, 1963). In addition, the regions which underly the protonosphere are heated by conduction from above where those photoelectrons which escape the F-region lose a large fraction of their energy. In the auroral and polar regions particle precipitation is also an important source of electron heating.

Whatever their source of heating, the thermal electrons lose energy by collisions with ions and neutrals in the atmosphere. In the process of cooling the electrons, the ion temperature,  $T_i$ , is elevated above the neutral gas temperature,  $T_g$ , although it does not necessarily reach  $T_e$ . Thus it is generally true in the ionosphere that  $T_e > T_i > T_g$ . At low altitudes where the ions are cooled very effectively by the neutral gas,  $T_i$  may approach  $T_g$ , although there is some evidence that this is not always true (Harris, et al, 1967). At higher altitudes ( $h > 300$  km) reduced cooling by the less abundant neutrals permits  $T_i$  to approach  $T_e$ . At the even higher altitudes of the measurements described here ( $h \gtrsim 1000$  km), heat transfer between the electron and ion populations becomes so small that heat conduction within the electron gas (Geisler and Bowhill, 1965) tends to control the electron temperature gradient. At these altitudes  $T_e$  and  $T_i$  may be significantly different but both will usually be elevated above  $T_g$ .

The Earth's magnetic field is a prime factor in controlling the thermal structure of the ionosphere. This control arises because both the heating by photoelectrons and the transport of heat by thermal conduction involve the motion

of charged particles parallel to the geomagnetic field. This simplifies the analysis, however, because one need not consider the energy balance of the entire ionosphere simultaneously. Instead attention can be limited to the energy balance within a single field tube at a time (Mayr, et al, 1967).

If one assumes that  $T_e \approx T_i$ , it is possible to obtain a rather simple form of electron energy equation which combines all of these processes for an electron-ion-neutral gas. In steady state,

$$3kN_e \frac{\partial T_e}{\partial t} = \kappa B \frac{\partial}{\partial s} \left( \frac{T_e^{5/2}}{B} \frac{\partial T_e}{\partial s} \right) + p N_e - \sum_{xy} \kappa_{x^+y} [x^+] [y] (T_e - T_g) = 0, \quad (4)$$

where

$\kappa$  = thermal conductivity coefficient along the field.

$B$  = magnetic field intensity

$s$  = distance along a field line

$p$  = photoelectron heat flux

$\kappa_{x^+y}$  = coefficients of cooling between ions  $x^+$  and neutrals  $y$ .

At any point along the field tube, the thermal electrons ( $N_e$ ) are heated by a flux of photoelectrons ( $p$ ) and cooled by a mixture of ions and neutrals ( $x^+$  and  $y$ ). The difference between the heating and cooling rates at each point is balanced by heat conduction into or away from that point.

### Latitudinal Structure of $T_e$

Consider for example a short field tube that intersects the equatorial plane at 1000 kilometers altitude. Electrons and ions are in good thermal contact along this entire field tube because of their large concentrations which enhance the local cooling. Furthermore, the ions and neutrals remain in good thermal contact even up to the top of the tube because of the effectiveness with which protons, the major ion, are cooled by hydrogen, the major neutral (Mayr et al, 1967).  $T_e$  may be rather large in the lower F-region where solar ultraviolet heating is greatest, but at higher altitudes along this short field tube local cooling returns the electron temperatures to values not much above the neutral temperature ( $T_e < 2 T_g$ ). Furthermore, the photoelectrons which escape the F-region suffer little loss of energy to the electrons along this tube because of its relatively small total electron content. Therefore much of the heat is dissipated in the lower F-region of the conjugate ionosphere.

The energy balance along middle latitude field tubes is quite different. The local cooling along the upper portion of these tubes (say  $L = 2-3$ ) is nearly negligible. Therefore, photoelectron heating produces an increasing temperature up to the equatorial crossing. The greater electron content of these tubes absorbs a larger fraction of the photoelectron energy so that less remains to heat the conjugate F-region. From this discussion one can understand qualitatively why  $T_e$  increases with latitude on the sunlit side of the Earth.

### Nightside $T_e$ at low latitudes

At night, the short field tubes at lower latitudes ( $<30^\circ$ ) cool rapidly by conduction to the lower ionosphere as well as locally by collisions with ions and neutrals. Therefore the slightly elevated temperatures observed within the equatorial trough (figures 4b and 5) are probably not produced primarily by heat conduction from the protonosphere. Indeed there is some probe evidence for slightly elevated temperatures in the equatorial F-region at night (Hanson et al, 1969). Radar backscatter measurements show lower values of  $T_e$  on these occasions. The radar cannot, of course, investigate the spatial variations suggested by probe observations (McClure, 1969).

The longitudinal and latitudinal structure of  $T_e$  evident at 1000 kilometers within the equatorial trough (4b and 5), are the best evidence that  $T_e$  is often elevated above  $T_g$  at night and is elevated by different degrees in different places. Although the uncertainty in  $T_g$  precludes our establishing an absolute value of the enhancements, it is probably safe to assume that  $T_g$  does not exhibit the degree of variation evident in  $T_e$  within the trough. Therefore we conclude that the variations in  $T_e$  reflect a source of heating with similar spatial, and probably temporal, variations.

Although one could argue that the probe measurements may yield values which are systematically high, we can identify no way in which the probes could find systematic latitude and longitude structure if it were not already present in the global structure of  $T_e$ . In the experimental frame of reference, each

orbit is like all others, except that the rotation of the Earth brings another longitude into the path of the satellite on consecutive orbits.

It should be noted that where probe and backscatter measurements of  $T_e$  disagree it is not yet possible to choose between them on geophysical grounds, as the sources of heating for the ionosphere are not known with sufficient precision. For example the probe values of  $T_e$  are consistent with a nocturnal source which is less than 1% of the daytime heating there. Such a source would only be evident in its effect upon  $T_e$ , a fact that emphasizes the value of such measurements for the detection of heat sources.

#### The Diurnal Variation of $T_e$ at Middle and High Latitudes

As shown earlier, the Explorer 22 and Alouette-II data show that  $T_e$  remains high throughout the night above  $L = 1.4$  so that considerably less diurnal variation in  $T_e$  is observed above this latitude, except in the polar region. Calculations show that the heat capacity of these longer field tubes is sufficient to preclude large variations in  $T_e$  in periods as short as a night (Nagy et al, 1968). If other nocturnal sources of electron heating are present, these may be masked at middle latitudes by heat conduction from the ever-hot protonosphere.

In the region encompassing the auroral zone ( $50^\circ$ - $70^\circ$ ) the diurnal variation of  $T_e$  is not well understood. Heat conduction from the protonosphere is complicated by the changing location of the plasmapause during periods of magnetic activity. One might therefore expect a corresponding equatorward movement of the nightside peak of  $T_e$ , normally seen at  $60^\circ$ . On the other hand, the

turbulent conditions which are responsible for the contraction of the plasma-pause may also be accompanied by other electron heating mechanisms.

The  $T_e$  behavior within the polar cap appears somewhat easier to understand. The slight elevation of  $T_e$  above  $T_g$  at night (polar winter) probably reflects heating by magnetospheric particles. The further elevation in  $T_e$  during the daytime (polar summer) results from solar heating. Perhaps the lack of a protonosphere above the polar cap explains why daytime temperatures do not reach middle latitude values.

#### Solar Cycle Variations in $T_e$

The changes in  $T_e$  within the solar cycle reflect basic changes in the electron thermal balance. Although increases in local and non-local electron heating are probably substantial, perhaps the greatest changes in  $T_e$  are induced by the changes in neutral and ion composition and their effect upon the electron cooling rates. A key factor is the loss of atomic hydrogen at elevated exospheric temperatures. At solar minimum, H and  $H^+$  are the major constituents at 1000 kilometers, except in the polar region where  $O^+$  predominates.  $H^+$  is effectively cooled by collisions with H, and electrons in turn are cooled by  $H^+$ . As the level of solar activity increases, the escape of H is accelerated and H -  $H^+$  cooling becomes less important at the altitudes of these measurements (1000-3000 km). At the same time photoelectron fluxes probably increase with solar activity, and the temperature throughout this altitude range increases. It should be noted that the loss of H -  $H^+$  cooling is partially compensated at lower altitudes ( $h < 1000$  km).

by increased concentrations of O which is also effective in cooling both H<sup>+</sup> and O<sup>+</sup>.

At still higher levels of solar activity, further increases in O concentration tend to reestablish the strong local cooling in the upper F-region and T<sub>e</sub> decreases, but not to the levels encountered at solar minimum. Brace, et al, (1968) have used this line of reasoning to explain the behavior of T<sub>e</sub> between 1965 and 1967.

#### CONCLUDING REMARKS

Although much has been learned over the past few years about the global variations of T<sub>e</sub>, the explanation of many aspects of this behavior remains largely speculation. And this will remain true until all of the various parameters which enter in the electron-ion-neutral heat budget can be observed simultaneously and in a reasonably comprehensive manner. Early satellites, such as those employed here, have combined measurements of several of the important parameters in the energy equation (4). However, the state of the art in the measurement of many other parameters has not yet permitted this goal to be achieved. Satellites currently being launched provide more comprehensive sets of measurements, but the broad scientific objectives of these missions often precludes the selection of orbits ideal for resolving aeronomics questions.

It is hoped that future satellites, now in the planning stage, will overcome many of these difficulties by combining the appropriate experiments on a satellite which has propulsion capability and which therefore can change its

eccentricity and altitudes many times in its lifetime. These spacecraft will be capable of exploiting all of the advantages of both eccentric and circular orbits and will do so in a controlled manner which permits definitive studies to be made.

#### ACKNOWLEDGEMENTS

I am grateful to G. R. Carignan and his associates at the University of Michigan Space Physics Research Laboratory for their excellent efforts in the design and fabrication of these experiments which have performed so reliably and thereby permitted the acquisition of the data presented here. I also thank J. A. Findlay of Goddard Space Flight Center for his efforts in the integration and preflight testing of the equipment.

## REFERENCES

- Brace, L. H. and P. L. Dyson, "Documentation of Explorer 32 electron temperature measurements used in comparisons with backscatter measurements at Jicamarca" Goddard Space Flight Center report X-621-68-469, Dec. 1968.
- Brace, L. H. and K. K. Mahajan, "Diurnal Variation in electron temperature in the equatorial protonosphere" (in preparation) 1969.
- Brace, L. H., H. G. Mayr and B. M. Reddy, "The early effects of increasing solar activity upon the temperature and density of the 1000-km ionosphere" J. Geophys. Res. 73, 1607, 1968.
- Brace, L. H. and B. M. Reddy, "Early electrostatic probe measurements from Explorer 22" J. Geophys. Res., 70, 5783, 1965.
- Brace, L. H., B. M. Reddy, and H. G. Mayr, "Global behavior of the ionosphere at 1000 km altitude" J. Geophys. Res. 72, 265, 1967.
- Donley, J. L. "Observations of the polar ionosphere in the range of 2000 to 3000 km by means of satellite-borne electron traps" Space Res., 8, 381, 1967.
- Evans, J. V. "Midlatitude F-region densities and temperatures at sunspot-minimum," Planet. Space Sci., 15, 1387, 1967.
- Findlay, J. A. and L. H. Brace, "Cylindrical electrostatic probes employed on Alouette-II and Explorer 31 satellites," IEEE Proceedings, June 1, 1969.
- Geisler, J. E., and S. A. Bowhill, "Exchange of energy between the ionosphere and the protonosphere" J. Atmospheric Terrest. Phys., 27, 1119, 1965.
- Hagg, E. L., "Electron densities of 8-100 'cc deduced from Alouette-II high-latitude ionograms" Canadian J. Physics, 45, 27, 1967.

Hanson, W. B., Space Research III (editor W. Priester) North Holland Pub. Co.,  
Amsterdam, 1963.

Hanson, W. B., L. H. Brace, P. L. Dyson and J. P. McClure, "Conflicting elec-  
tron temperature measurements in the upper F-region," J. Geophys. Res.  
74, 400, 1969.

Harris, K. K., G. W. Sharp and W. C. Knudson, "Ion temperatures and relative  
ion composition measurements from a low altitude polar-orbiting-satellite,"  
J. Geophys. Res. 72, 5039, 1967.

Jacchia, L. G., "The temperature above the thermopause," Smithsonian Astro-  
physical Observatory Report No. 150, April 1964.

Mahajan, K. K., and L. H. Brace, "Global observations on the thermal balance  
of the night time protonosphere," Goddard Space Flight Center Report X-621-  
68-508, 1968, (accepted J. Geophys. Res.), 1968.

Mayr, H. G., L. H. Brace, and G. S. Dunham, "Ion composition and temperature  
in the topside ionosphere," J. Geophys. Res. 72, 4391, 1967.

McClure, J. P., "The diurnal variation of neutral and charged particle tem-  
peratures in the equatorial F-region," J. Geophys. Res., 74, 279, 1969.

Muldrew, D. B., "F-layer ionization troughs deduced from Alouette I data,"  
J. Geophys. Res., 70, 2635, 1965.

Nagy, A. F., P. Bauer and E. G. Fontheim, "Nighttime cooling of the protonosphere"  
J. Geophys. Res. 73, 6259, 1968.

Willmore, A. P., "Geophysical and solar activity variations in the electron  
temperature of the upper F-region," Proc. Roy. Soc., London A 286, 537,  
1965.